Contribution from the Department of Chemistry and Biochemistry, University of Colorado, Boulder, Colorado 80309

Charge Delocalization in Ruthenium–Quinone Complexes. Structural Characterization of Bis(bipyridine)(3,5-di-*tert*-butylsemiquinonato)ruthenium(II) Perchlorate and *trans*-Bis(4-*tert*-butylpyridine)bis(3,5-di-*tert*-butylquinone)ruthenium

Steven R. Boone and Cortlandt G. Pierpont*

Received November 13, 1986

Two complexes of ruthenium containing 3,5-di-*tert*-butylquinone ligands have been characterized crystallographically. The perchlorate salt of bis(bipyridine)(3,5-di-*tert*-butylsemiquinonato)ruthenium(II), $[Ru(bpy)_2(DBSQ)]ClO_4$, crystallizes in the monoclinic space group $P2_1/c$ with a = 15.361 (2) Å, b = 24.229 (3) Å, c = 11.026 (2) Å, β = 103.51 (1)°, and Z = 4. The complex cation is octahedral in structure, with Ru–O and Ru–N lengths that are typical of Ru(II) and Ru(III) complexes. Structural features of the quinone ligand show one C–O length with a value found typically for semiquinones and the second length to be slightly longer. *trans*-Bis(4-*tert*-butylpyridine)bis(3,5-di-*tert*-butylquinone)ruthenium, $Ru(4\text{-}t\text{-}Bupy)_2(DBQ)_2$, crystallizes in the triclinic space group $P\bar{1}$ with a = 9.072 (2) Å, b = 11.068 (2) Å, c = 11.554 (2) Å, α = 90.25 (2)°, β = 99.51 (2)°, γ = 95.96 (2)°, and Z = 1 with crystallographic inversion symmetry imposed on the molecule. Bond lengths to the metal fail to provide information on the charge distribution within the molecule. Quinone C–O lengths are intermediate between catecholate and semiquinonate values, suggesting charge delocalization within the ruthenium–quinone chelate ring.

Introduction

Charge distribution in transition-metal–quinone complexes is dependent upon the relative values of metal and quinone orbital energies. In complexes where metal electronic levels are on the same order of energy as the quinone π^* level, the ligands bond with partially oxidized metals in the semiquinone form. This has been found to be the case in neutral, binary complexes of first-row transition metals, $M(SQ)_{2,3}$, prepared with metals ranging across the first transition series from V to Cu.[1-7] Related complexes containing second- and third-row metals appear to consist of fully oxidized metal ions chelated by catecholate ligands, although the chemistry of quinone complexes of the larger metals has not been developed to the extent of that of the first-row metals. Specific examples for comparison exist in the Cr, Mo, W triad where the chromium complexes are of the form $Cr^{III}(SQ)_3$ while complexes of the larger metals contain hexavalent metals bonded by catecholate ligands, $M^{VI}(Cat)_3$.[8-12] Similarly, the manganese complex prepared with 3,5-di-*tert*-butyl-1,2-benzoquinone contains Mn(II) in a tetrameric molecule, $[Mn^{II}(DBSQ)_2]_4$, while with rhenium the complex contains Re(VI) in $Re^{VI}(DBCat)_3$.[3,13] Within the iron triad the results are somewhat less clear. With various spectroscopic, magnetic, and structural methods the iron complexes have been shown to be of the form $Fe^{III}(SQ)_3$, in accord with other first-row metals.[4] However, the osmium analogues, from structural characterization, fail to show the clear features of catecholate coordination found with Mo and Re.[12] This has suggested that the charge distribution found in complexes of the larger metals of the iron triad may be less clearly defined than structural results have indicated on virtually all other complexes of semiquinonate and catecholate ligands.

Table I. Crystal Data and Details of the Structure Determination for $[Ru(bpy)_2(DBSQ)]ClO_4$

Crystal Data			
formula	$RuClO_6N_4C_{34}H_{36}$	V, Å^3	3990.1 (3)
M_r	733.19	Z	4
space group[a]	$P2_1/c$	d_{calcd}, g cm^{-3}	1.220
cryst syst	monoclinic	d_{exptl}, g cm^{-3}	1.22 (2)
a,[b] Å	15.361 (2)	F(000)	1508
b, Å	24.229 (3)	μ, cm^{-1}	4.92
c, Å	11.026 (2)	cryst dimens, mm	0.32 × 0.27 × 0.18
β, deg	103.51 (1)		

Data Collection and Reduction	
diffractometer	Syntex P$\bar{1}$
data collcd	$+h,+k,\pm l$
radiation (λ, Å)	Mo Kα (0.71069)
monochromator angle, deg	12.2
temp, K	294–296
scan technique	θ–2θ
scan range (2θ) min–max, deg	3.0–45.0
scan speed, deg/min	4.0
scan range, deg	0.7 below Kα_1 and 0.7 above Kα_2
bkgd	stationary cryst–stationary counter bkgd time = 0.5(scan time)
no. of unique reflcns measd	5426
no. of obsd reflcns criterion	2576 $F > 6\sigma(F)$

Structure Determination and Refinement	
programs used	SHELX[c]
scattering factors	neutral atoms[d]
R_1, R_2[e]	0.059, 0.068
wt	$1/(\sigma(F)^2 + 0.0005F^2)$
no. of params	415
ratio of observns to params	6.2
max shift/error (non-hydrogen)	0.043
residual electron density, e/Å^3	2.2

[a] *International Tables for X-ray Crystallography*; Kynoch; Birmingham, England, 1965; Vol. 1. [b] Cell dimensions were determined by least-squares fit of the setting angles of 21 reflections with 2θ in the range 10–25°. [c] Sheldrick, G. M. "SHELX76, A Program for Crystal Structure Determination", University of Cambridge: Cambridge, England. [d] *International Tables for X-ray Crystallography*; Kynoch: Birmingham, England, 1974; Vol. 4, pp 55–60, 99–101, 149–150. [e] The quantity minimized in the least-squares procedures is $\sum w(|F_o| - |F_c|)^2$. $R_1 = \sum||F_o| - |F_c||/\sum|F_o|$. $R_2 = [\sum w(|F_o| - |F_c|)^2/\sum w(F_o)^2]^{1/2}$.

Lever and co-workers have recently reported a series of ruthenium–quinone complexes that also contain nitrogen donor ligands. Spectral characterization on several examples of this series failed to provide results consistent with a clear charge distribution.[14,15] Herein we report structural characterization on mono-

(1) (a) Cass, M. E.; Greene, D. L.; Buchanan, R. M.; Pierpont, C. G. *J. Am. Chem. Soc.* **1983**, *105*, 2680. (b) Cass, M. E.; Gordon, N. R.; Pierpont, C. G. *Inorg. Chem.* **1986**, *25*, 3962.
(2) Buchanan, R. M.; Kessel, S. L.; Downs, H. H.; Pierpont, C. G.; Hendrickson, D. N. *J. Am. Chem. Soc.* **1978**, *100*, 7894.
(3) Lynch, M. W.; Hendrickson, D. N.; Fitzgerald, B. J.; Pierpont, C. G. *J. Am. Chem. Soc.* **1984**, *106*, 2041.
(4) Cohn, M. J.; Xie, C.-L.; Tuchagues, J.-P. M.; Pierpont, C. G.; Hendrickson, D. N. *J. Am. Chem. Soc.*, in press.
(5) Buchanan, R. M.; Fitzgerald, B. J.; Pierpont, C. G. *Inorg. Chem.* **1979**, *18*, 3439.
(6) Lynch, M. W.; Buchanan, R. M.; Pierpont, C. G.; Hendrickson, D. N. *Inorg. Chem.* **1981**, *20*, 1038.
(7) (a) Abakumov, G. A.; Lobanov, A. V.; Cherkasov, V. K.; Razuvaev, G. A. *Inorg. Chim. Acta* **1981**, *49*, 135. (b) Thompson, J. S.; Calabrese, J. C. *J. Am. Chem. Soc.* **1986**, *108*, 1903.
(8) Pierpont, C. G.; Downs, H. H. *J. Am. Chem. Soc.* **1975**, *97*, 2123.
(9) Pierpont, C. G.; Buchanan, R. M. *J. Am. Chem. Soc.* **1975**, *97*, 4912.
(10) Pierpont, C. G.; Downs, H. H.; Buchanan, R. M. *J. Am. Chem. Soc.* **1974**, *96*, 5573.
(11) Beshouri, S. M.; Rothwell, I. P. *Inorg. Chem.* **1986**, *25*, 1962.
(12) Nielson, A. J.; Griffith, W. P. *J. Chem. Soc., Dalton Trans.* **1978**, 1501.
(13) de Learie, L. A.; Pierpont, C. G. *J. Am. Chem. Soc.* **1986**, *108*, 6393.
(14) Haga, M.-A.; Dodsworth, E. S.; Lever, A. B. P. *Inorg. Chem.* **1986**, *25*, 447.

0020-1669/87/1326-1769$01.50/0

Table II. Atomic Positional and Derived Isotropic Thermal Parameters for $[Ru(bpy)_2(DBSQ)](ClO_4)$

atom	x	y	z	U,[a] Å^2
Ru	0.23655 (6)	0.04544 (4)	0.06007 (9)	0.0379 (5)
O1	0.2858 (5)	0.1114 (3)	−0.0157 (7)	0.030 (5)
O2	0.1490 (5)	0.1048 (3)	0.0904 (7)	0.040 (5)
C1	0.2345 (8)	0.1541 (5)	−0.026 (1)	0.043 (8)
C2	0.1586 (8)	0.1511 (5)	0.031 (1)	0.038 (7)
C3	0.0979 (8)	0.1959 (5)	0.028 (1)	0.047 (8)
C4	0.1111 (8)	0.2432 (5)	−0.036 (1)	0.048 (8)
C5	0.1857 (9)	0.2465 (5)	−0.098 (1)	0.053 (8)
C6	0.2461 (8)	0.2035 (5)	−0.094 (1)	0.045 (7)
C7	0.0464 (9)	0.2931 (5)	−0.043 (1)	0.065 (9)
C8	0.3261 (8)	0.2091 (5)	−0.154 (1)	0.055 (8)
C9	0.036 (1)	0.3074 (7)	0.085 (2)	0.14 (1)
C10	0.080 (1)	0.3448 (7)	−0.094 (2)	0.16 (1)
C11	−0.043 (1)	0.2774 (8)	−0.120 (2)	0.15 (1)
C12	0.322 (1)	0.2631 (6)	−0.229 (1)	0.08 (1)
C13	0.3309 (8)	0.1590 (6)	−0.239 (1)	0.06 (1)
C14	0.4120 (8)	0.2112 (6)	−0.044 (1)	0.07 (1)
N1	0.3279 (6)	0.0575 (4)	0.2262 (9)	0.040 (6)
N2	0.3370 (6)	−0.0069 (4)	0.038 (1)	0.045 (6)
C15	0.3140 (9)	0.0902 (5)	0.318 (1)	0.061 (9)
C16	0.382 (1)	0.0989 (6)	0.426 (1)	0.073 (9)
C17	0.465 (1)	0.0725 (7)	0.437 (1)	0.082 (9)
C18	0.4775 (9)	0.0383 (6)	0.342 (1)	0.075 (9)
C19	0.4062 (8)	0.0303 (5)	0.238 (1)	0.048 (8)
C20	0.4120 (8)	−0.0068 (5)	0.135 (1)	0.056 (9)
C21	0.4863 (8)	−0.0403 (7)	0.131 (2)	0.078 (9)
C22	0.481 (1)	−0.0750 (7)	0.026 (2)	0.093 (10)
C23	0.405 (1)	−0.0735 (6)	−0.069 (2)	0.077 (10)
C24	0.3335 (8)	−0.0403 (6)	−0.062 (1)	0.063 (8)
N3	0.1444 (6)	0.0244 (4)	−0.1009 (9)	0.038 (5)
N4	0.1758 (6)	−0.0215 (4)	0.119 (1)	0.041 (6)
C25	0.0866 (8)	−0.0159 (5)	−0.090 (1)	0.045 (7)
C26	0.0155 (7)	−0.0331 (5)	−0.188 (1)	0.051 (8)
C27	0.0053 (8)	−0.0044 (6)	−0.301 (1)	0.052 (8)
C28	0.0638 (8)	0.0373 (6)	−0.318 (1)	0.058 (9)
C29	0.1328 (7)	0.0522 (5)	−0.215 (1)	0.050 (8)
C30	0.1068 (7)	−0.0438 (5)	0.032 (1)	0.042 (6)
C31	0.0590 (8)	−0.0900 (5)	0.062 (1)	0.059 (9)
C32	0.0834 (9)	−0.1131 (5)	0.178 (1)	0.067 (9)
C33	0.1572 (9)	−0.0898 (6)	0.267 (1)	0.065 (10)
C34	0.2000 (7)	−0.0440 (6)	0.234 (1)	0.049 (8)
C1	0.2611 (2)	−0.0128 (2)	0.5749 (4)	0.082 (3)
O3	0.3186 (6)	−0.0368 (5)	0.5030 (9)	0.109 (8)
O4	0.3112 (6)	0.0191 (5)	0.6756 (9)	0.106 (8)
O5	0.1992 (6)	0.0229 (5)	0.496 (1)	0.124 (9)
O6	0.2154 (9)	0.0537 (6)	0.626 (1)	0.167 (10)

[a] Equivalent isotropic U defined as one-third of the trace of the orthogonalized U_{ij} tensor.

and bis(quinone) complexes of ruthenium in an attempt to resolve questions concerning formal assignment of charge. The two complexes included in this study are $[Ru(bpy)_2(DBSQ)](ClO_4)$ and $Ru(4\text{-}t\text{-}Bupy)_2(DBQ)_2$.[16]

Experimental Section

Crystals used in this investigation were provided by Prof. A. B. P. Lever, York University, Downsview, Ontario and by Prof. Masa-aki Haga, Mie University, Mie, Japan.

Structure Determination of $[Ru(bpy)_2(DBSQ)](ClO_4)$. A black-brown crystal of $[Ru(bpy)_2(DBSQ)](ClO_4)$ suitable for crystallographic analysis was mounted and aligned on a Syntex $P\bar{1}$ automated diffractometer. Crystal quality was examined by using rotational and axial photographs and judged satisfactory for data collection. Information regarding data collection and structure determination is given in Table I. Four standard reflections measured during data collection showed only statistical fluctuations in intensity. Experiments carried out to estimate the effect of absorption indicated that correction was unnecessary. The location of the ruthenium atom was determined from a Patterson map; the locations of other atoms were determined from phases generated by using the Ru atom position. Fixed contributions for all hydrogen atoms were included in final cycles of refinement. All non-hydrogen atoms of the structure were refined with anisotropic thermal parameters. The largest parameter shifts on the final cycle of refinement occurred for the thermal parameters of perchlorate oxygen O6, and the greatest residual electron density was in the vicinity of the perchlorate oxygens. Final atomic coordinates for $[Ru(bpy)_2(DBSQ)](ClO_4)$ are given in Table II. Tables containing anisotropic thermal parameters and structure factors are available as supplementary material.

Table III. Crystal Data and Details of the Structure Determination for $Ru(t\text{-}Bupy)_2(DBQ)_2$

Crystal Data			
formula	$RuO_4N_2C_{46}H_{66}$	β, deg	99.51 (2)
M_r	811.58	γ, deg	95.96 (2)
space group[a]	$P\bar{1}$	V, Å^3	1137.7 (3)
cryst syst	triclinic	Z	1
a,[b] Å	9.072 (2)	d_{calcd}, g cm^{-3}	1.185
b, Å	11.068 (2)	d_{exptl}, g cm^{-3}	1.17 (2)
c, Å	11.554 (2)	$F(000)$	432
α, deg	90.25 (2)	μ, cm^{-1}	3.75
		cryst dimens, mm	0.47 × 0.38 × 0.31

Data Collection and Reduction	
diffractometer	Syntex $P\bar{1}$
data collcd	$+h,\pm k,\pm l$
radiation (λ, Å)	Mo Kα (0.710 69)
monochromator angle, deg	12.2
temp, K	294–296
scan technique	θ–2θ
scan range (2θ) min–max, deg	3.0–50.0
scan speed, deg/min	4.0
scan range, deg	0.7 below $K\alpha_1$ and 0.7 above $K\alpha_2$
bkgd	stationary cryst–stationary counter bkgd time = 0.5(scan time)
no. of unique reflcns measd	4536
no. of obsd reflcns	3918
criterion	$F > 6\sigma(F)$

Structure Determination and Refinement	
programs used	SHELX[c]
scattering factors	neutral atoms[d]
R_1, R_2[e]	0.048, 0.059
wt	$1/(\sigma(F)^2 + 0.0005F^2)$
no. of params	241
ratio of observns to params	16.3
max shift/error (non-hydrogen)	0.023
residual electron density, e/Å^3	1.8

[a] *International Tables for X-ray Crystallography*; Kynoch: Birmingham, England, 1965; Vol. 1. [b] Cell dimensions were determined by least-squares fit of the setting angles of 15 reflections with 2θ in the range 20–30°. [c] Sheldrick, G. M. "SHELX76, A Program for Crystal Structure Determination", University of Cambridge: England. [d] *International Tables for X-ray Crystallography*; Kynoch: Birmingham, England, 1974; Vol. 4, pp 55–60, 99–101, 149–150. [e] The quantity minimized in the least-squares procedures is $\sum w(|F_o| - |F_c|)^2$. $R_1 = \sum||F_o| - |F_c||/\sum|F_o|$. $R_2 = [\sum w(|F_o| - |F_c|)^2/\sum w(F_o)^2]^{1/2}$.

Structure Determination of $Ru(4\text{-}t\text{-}Bupy)_2(DBQ)_2$. A black-brown crystal of the complex was mounted and aligned on the diffractometer as in the previous structure determination. Crystallographic information for $Ru(4\text{-}t\text{-}Bupy)_2(DBQ)_2$ is given in Table III. With one molecule per unit cell in the triclinic crystal system, the ruthenium atom was placed at the origin and the locations of other atoms of the centrosymmetric molecule were determined from phases generated from this atom position. All non-hydrogen atoms of the structure were refined with anisotropic thermal parameters. The largest parameter shifts on the final cycle of refinement occurred for the thermal parameters of quinone *tert*-butyl carbon atom C14, and the greatest residual electron density was in the vicinity of the quinone *tert*-butyl including carbon C11. Final atomic coordinates for $Ru(4\text{-}t\text{-}Bupy)_2(DBQ)_2$ are given in Table IV. Tables containing anisotropic thermal parameters and structure factors are available as supplementary material.

Results

Description of $[Ru(bpy)_2(DBSQ)](ClO_4)$. Often metal–ligand bond lengths provide insights on metal ion charge, but such is not

(15) (a) Haga, M.-A.; Dodsworth, E. S.; Lever, A. B. P.; Boone, S. R.; Pierpont, C. G. *J. Am. Chem. Soc.* **1986**, *108*, 7321. (b) Haga, M.-A.; Nevin, W. A.; Liu, W.; Dodsworth, E. S.; Melnick, M.; Lever, A. B. P., submitted for publication.

(16) The term *quinone* is used without reference to ligand charge as it appears as a root in the names of all three electronic forms, benzo*quinone*, semi*quinone*, and hydro*quinone* (catechol).

Table IV. Atomic Positional and Derived Isotropic Thermal Parameters for $Ru(t\text{-}Bupy)_2(DBQ)_2$

atom	*x*	*y*	*z*	U,[a] Å^2
Ru	0	0	0	0.0381 (2)
O1	−0.0673 (3)	0.1364 (2)	−0.1001 (2)	0.042 (1)
O2	0.1013 (3)	−0.0283 (2)	−0.1371 (2)	0.048 (1)
C1	0.0037 (4)	0.1535 (3)	−0.1907 (3)	0.038 (2)
C2	0.0974 (5)	0.0631 (3)	−0.2102 (3)	0.041 (2)
C3	0.1743 (5)	0.0691 (4)	−0.3053 (4)	0.050 (2)
C4	0.1571 (5)	0.1634 (4)	−0.3836 (4)	0.053 (2)
C5	0.0624 (5)	0.2524 (4)	−0.3638 (4)	0.051 (2)
C6	−0.0155 (5)	0.2494 (4)	−0.2705 (3)	0.043 (2)
C7	0.2355 (6)	0.1750 (5)	−0.4911 (4)	0.067 (3)
C8	0.330 (1)	0.0697 (8)	−0.5017 (8)	0.181 (8)
C9	0.3395 (7)	0.2972 (7)	−0.4806 (6)	0.099 (4)
C10	0.1170 (9)	0.1857 (8)	−0.6011 (5)	0.105 (5)
C11	−0.1212 (6)	0.3454 (4)	−0.2532 (4)	0.056 (2)
C12	−0.0671 (6)	0.4094 (4)	−0.1313 (5)	0.067 (2)
C13	−0.2840 (6)	0.2810 (5)	−0.2587 (6)	0.078 (3)
C14	−0.1216 (8)	0.4447 (6)	−0.3486 (5)	0.095 (4)
N	0.1966 (4)	0.1071 (3)	0.0702 (3)	0.043 (1)
C15	0.1987 (5)	0.2267 (4)	0.0906 (4)	0.052 (2)
C16	0.3305 (5)	0.3006 (4)	0.1302 (5)	0.056 (2)
C17	0.4670 (5)	0.2533 (4)	0.1513 (4)	0.050 (2)
C18	0.4624 (5)	0.1276 (4)	0.1303 (5)	0.066 (2)
C19	0.3278 (6)	0.0598 (4)	0.0910 (5)	0.063 (2)
C20	0.6159 (5)	0.3308 (4)	0.1923 (5)	0.063 (2)
C21	0.6896 (9)	0.2797 (8)	0.3143 (8)	0.121 (5)
C22	0.5987 (8)	0.4616 (7)	0.210 (1)	0.146 (3)
C23	0.722 (1)	0.3131 (8)	0.1067 (9)	0.152 (5)

[a] Equivalent isotropic U defined as one-third of the trace of the orthogonalized U_{ij} tensor.

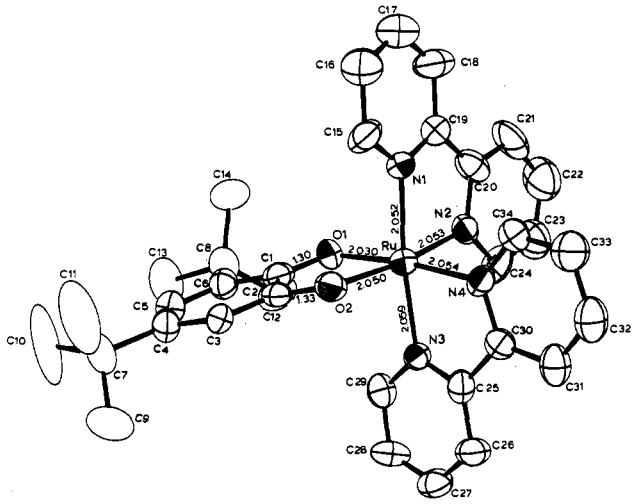

Figure 1. ORTEP plot showing a view of the $Ru(bpy)_2(DBSQ)^+$ cation and the atom-numbering scheme.

the case with ruthenium. Structures of $Ru(bpy)_2Cl_2$ and $Ru(bpy)_2Cl_2^+$ reported recently by Meyer, Hodgson, and co-workers clearly illustrate this point.[17] Ruthenium–nitrogen lengths for Ru–N bonds trans to one another differ insignificantly, 2.054 Å for Ru(II) and 2.060 Å for Ru(III). Bond lengths at positions that are trans to atoms other than bipyridine nitrogens are more sensitive to π-bonding effects than to metal atom charge. This is apparent in the structure of *cis*-$Ru(bpy)_2(CO)Cl$ where the Ru–N length trans to the carbonyl ligand is 0.1 Å longer than the length at the position trans to the Ru–Cl bond.[18]

There is no significant variation in the Ru–N bond lengths of the $Ru(bpy)_2(DBSQ)^+$ cation, and the average value of 2.054 Å does not allow distinction between Ru(II) and Ru(III). A view of the complex cation is shown in Figure 1, and bond distances and angles are given in Table V. The similarity of lengths at positions trans to other bipyridine nitrogens and trans to quinone oxygens leads to the conclusion that bonding effects of both ligands are quite similar. Quinone C–O lengths have proven to be sensitive to quinone charge in other structure determinations. Catecholate ligands have been found to have C–O lengths of 1.34 (1) Å and

Table V. Bond Distances and Selected Bond Angles for $[Ru(bpy)_2(DBSQ)](ClO_4)$

Interatomic Distances (Å)			
Ru–O1	2.030 (0.008)	Ru–O2	2.050 (0.008)
Ru–N1	2.052 (0.009)	Ru–N2	2.054 (0.010)
Ru–N3	2.059 (0.008)	Ru–N4	2.054 (0.010)
O1–C1	1.289 (0.014)	O2–C2	1.327 (0.015)
C1–C2	1.445 (0.018)	C1–C6	1.446 (0.017)
C2–C3	1.426 (0.017)	C3–C4	1.388 (0.018)
C4–C5	1.463 (0.021)	C4–C7	1.555 (0.018)
C5–C6	1.388 (0.018)	C6–C8	1.537 (0.019)
C7–C9	1.503 (0.025)	C7–C10	1.509 (0.024)
C7–C11	1.486 (0.020)	C8–C12	1.541 (0.019)
C8–C13	1.547 (0.019)	C8–C14	1.569 (0.016)
N1–C15	1.345 (0.017)	N1–C19	1.351 (0.015)
N2–C20	1.379 (0.014)	N2–C24	1.358 (0.017)
C15–C16	1.404 (0.018)	C16–C17	1.405 (0.023)
C17–C18	1.379 (0.023)	C18–C19	1.403 (0.017)
C19–C20	1.463 (0.019)	C20–C21	1.411 (0.019)
C21–C22	1.414 (0.025)	C22–C23	1.373 (0.021)
C23–C24	1.380 (0.021)	N3–C25	1.344 (0.015)
N3–C29	1.396 (0.016)	N4–C30	1.363 (0.013)
N4–C34	1.350 (0.016)	C25–C26	1.406 (0.016)
C25–C30	1.478 (0.017)	C26–C27	1.404 (0.019)
C27–C28	1.394 (0.019)	C28–C29	1.412 (0.015)
C30–C31	1.418 (0.018)	C31–C32	1.372 (0.020)
C32–C33	1.430 (0.018)	C33–C34	1.381 (0.020)
C1–O3	1.440 (0.012)	C1–O4	1.423 (0.011)
C1–O5	1.425 (0.012)	C1–O6	1.409 (0.016)
Selected Angles (deg)			
O2–Ru–O1	80.6 (0.3)	N1–Ru–O1	90.7 (0.3)
N1–Ru–O2	95.3 (0.3)	N2–Ru–O1	94.3 (0.3)
N2–Ru–O2	172.7 (0.3)	N2–Ru–N1	79.5 (0.4)
N3–Ru–O1	95.0 (0.3)	N3–Ru–O2	88.3 (0.3)
N3–Ru–N1	173.7 (0.4)	N3–Ru–N2	97.5 (0.4)
N4–Ru–O1	173.8 (0.3)	N4–Ru–O2	98.0 (0.4)
N4–Ru–N1	95.5 (0.4)	N4–Ru–N2	87.7 (0.4)
N4–Ru–N3	78.8 (0.4)	C1–O1–Ru	112.8 (0.7)
C2–O2–Ru	111.0 (0.7)	C2–C1–O1	117.5 (1.1)
C6–C1–O1	124.2 (1.1)	C6–C1–C2	118.2 (1.1)
C1–C2–O2	116.7 (1.0)	C3–C2–O2	120.3 (1.1)
C3–C2–C1	122.9 (1.1)	C15–N1–Ru	124.2 (0.8)
C19–N1–Ru	115.1 (0.8)	C19–N1–C15	120.7 (1.0)
C20–N2–Ru	115.0 (0.8)	C24–N2–Ru	125.1 (0.7)
C24–N2–C20	119.9 (1.0)	C25–N3–Ru	116.1 (0.8)
C29–N3–Ru	124.9 (0.7)	C30–N4–Ru	115.2 (0.8)
C34–N4–Ru	124.8 (0.7)		

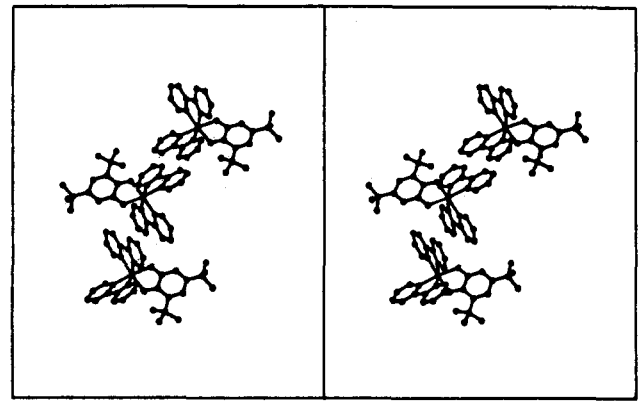

Figure 2. Stereoview showing interactions between complex cations in the crystal structure of $[Ru(bpy)_2(DBSQ)]ClO_4$. The strongest interaction between bipyridine ligands is shown at the lower part of the view. The ClO_4^- anions have been omitted for clarity.

(17) Eggleston, D. S.; Goldsby, K. A.; Hodgson, D. J.; Meyer, T. J. *Inorg. Chem.* **1985**, *24*, 4573.

(18) (a) Clear, J. M.; Kelly, J. M.; O'Connell, C. M.; Vos, J. G.; Cardin, C. J.; Costa, S. R.; Edwards, A. J. *J. Chem. Soc., Chem. Comm.* **1980**, 750. (b) McMillan, R. S.; Mercer, A.; James, B. R.; Trotter, J. *J. Chem. Soc., Dalton Trans.* **1975**, 1006.

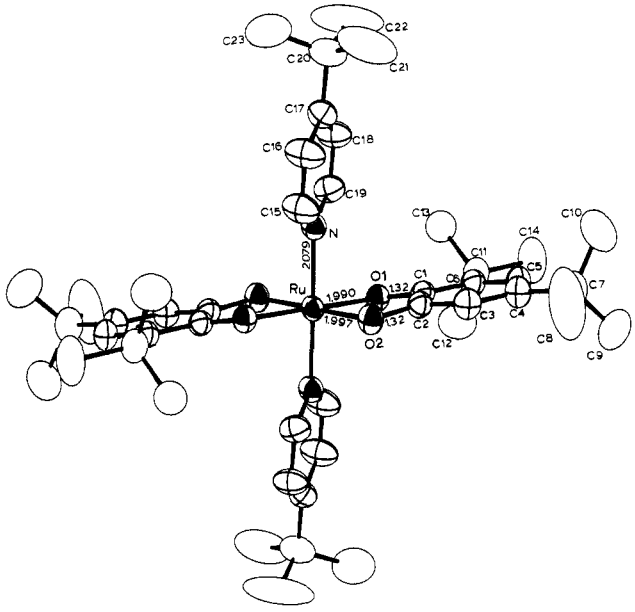

Figure 3. ORTEP plot showing a view of $Ru(4\text{-}t\text{-}Bupy)_2(DBQ)_2$ and the atom-numbering scheme.

semiquinonates have lengths of 1.29 (1) Å in a large number of structure determinations on quinone complexes. Quinone C–O lengths of $Ru(bpy)_2(DBSQ)^+$ are 1.289 (14) Å for C1–O1, quite consistent with the semiquinonate value, and 1.327 (15) Å for C2–O2, close to the catecholate value. Other structural features of the ligands are unexceptional and provide no further information on the charge distribution within the complex.

The crystal structure of the complex, shown in Figure 2, may provide some insight into the asymmetry of the quinone ligand structure. Bipyridine ligands of adjacent complex molecules stack to form a one-dimensional chain of cations in the crystal structure. The interaction between adjacent bipyridine ligands containing nitrogens N1 and N2, atoms that are both cis to O1 and close to the *tert*-butyl group at the ring 3-position of the quinone, is a relatively weak "slipped stacking interaction". While the bipyridine ligands of adjacent molecules are parallel, only the outer atoms are in close proximity, and better parallel overlap is prohibited by the presence of the *tert*-butyl group of the adjacent molecule. Overlap between ligands containing N3 and N4 is much more direct in the absence of steric interference. The separation between ligand planes is 3.5 Å, and the closest interatomic separation between bipyridine atoms is 3.46 Å between C25 and C31 of the corresponding ligand related by the inversion center at the origin of the unit cell. The closest interionic contacts occur between bipyridine carbon atoms C26′ and C31′ and oxygen O2 of the adjacent molecule. Carbon–oxygen contacts between these atoms are 3.26 and 3.44 Å, and the hydrogen atoms bonded to these carbons are directed toward the oxygen. This interaction may contribute to the asymmetry in ligand bonding. The difference in C–O bond lengths found in this structure determination has been observed for semiquinonate ligands in other structure determinations, but in situations where quinone oxygen atoms bridge adjacent metal atoms.[5]

Description of *trans*-$Ru(4\text{-}t\text{-}Bupy)_2(DBQ)_2$. The neutral $Ru(4\text{-}t\text{-}Bupy)_2(DBQ)_2$ complex molecule is located about a crystallographic inversion center in the unit cell. A view of the molecule is shown in Figure 3; bond distances and angles are given in Table VI. Ruthenium–nitrogen bond lengths to the *tert*-butylpyridine ligand are 2.079 (3) Å, approximately 0.03 Å longer than trans Ru–N lengths of the previous structure. Ruthenium–oxygen lengths average 1.994 (3) Å, 0.04 Å shorter than Ru–O lengths in $Ru(bpy)_2(DSQ)^+$ and shorter than the 2.028 (4) Å average Ru–O length of $Ru(O_2C_2O_2)^{3-}$[19]. This value remains

(19) Faure, R.; Duc, G.; Deloume, J.-P.; *Acta Crystallogr., Sect. C.*: **1986**, *C42*, 982.

Table VI. Bond Distances and Selected Bond Angles for $Ru(t\text{-}Bupy)_2(DBQ)_2$

Interatomic Distances (Å)			
Ru–O1	1.990 (0.003)	Ru–O2	1.997 (0.003)
Ru–N	2.079 (0.003)	O1–C1	1.322 (0.005)
O2–C2	1.320 (0.005)	C1–C2	1.419 (0.005)
C1–C6	1.414 (0.005)	C2–C3	1.395 (0.006)
C3–C4	1.388 (0.006)	C4–C5	1.415 (0.006)
C4–C7	1.530 (0.006)	C5–C6	1.381 (0.006)
C6–C11	1.537 (0.006)	C7–C8	1.532 (0.008)
C7–C9	1.559 (0.008)	C7–C10	1.537 (0.008)
C11–C12	1.555 (0.007)	C11–C13	1.564 (0.007)
C11–C14	1.559 (0.006)	N–C15	1.341 (0.005)
N–C19	1.336 (0.006)	C15–C16	1.386 (0.006)
C16–C17	1.379 (0.006)	C17–C18	1.406 (0.006)
C17–C20	1.526 (0.006)	C18–C19	1.372 (0.007)
C20–C21	1.590 (0.009)	C20–C22	1.489 (0.008)
C20–C23	1.514 (0.008)		
Selected Angles (deg)			
O2–Ru–O1	80.5 (0.1)	N–Ru–O1	90.3 (0.1)
N–Ru–O2	86.1 (0.1)	Cu–O1–Ru	113.3 (0.2)
C2–O2–Ru	112.6 (0.2)	C2–C1—O1	115.5 (0.3)
C6–C1–O1	124.6 (0.3)	C6–C1–C2	119.7 (0.3)
C1–C2–O2	116.4 (0.3)	C3–C2–O2	122.7 (0.3)
C3–C2–C1	120.9 (0.3)	C15–N–Ru	121.8 (0.3)
C19–N–Ru	120.7 (0.3)		

0.02 Å longer than the 1.974 (4) Å value reported for *trans*-dichlorobis(triazine 1-oxidato)ruthenium(IV), however.[20] A decrease in Ru–O bond length might be expected to occur with an increase in metal charge due to more favorable catecholate–metal π bonding. As before, metal–ligand bond lengths provide little direct information on metal ion charge. The quinone C–O lengths are 1.321 (5) Å, a value intermediate between lengths associated with semiquinonate and catecholate ligands, and other structural features of the ligands are unexceptional. With *tert*-butyl groups on both the pyridine and quinone ligands, there are no close intermolecular contacts in the crystal structure. The molecular structure of $Ru(4\text{-}t\text{-}Bupy)_2(DBQ)_2$ closely resembles that of *trans*-$Mn(py)_2(DBCat)_2$ containing Mn(IV), with the difference that quinone C–O lengths in the manganese case are clearly catecholate in value (1.349 (4) Å).[3]

Charge Distribution in $Ru(bpy)_2(DBSQ)^+$ and $Ru(4\text{-}t\text{-}Bupy)_2(DBQ)_2$. Restricting charge on the quinone ligands to either semiquinone or catecholate, a number of representations that differ in charge distribution between quinone and metal can be written for these complexes. The $Ru(bpy)_2(DBQ)^+$ cation could either contain Ru(II) as $Ru^{II}(bpy)_2(DBSQ)^+$ or Ru(III) as $Ru^{III}(bpy)_2(DBCat)^+$, with a shift in the paramagnetic center from ligand to metal. This shift should result in a marked change in the EPR spectrum as observed for the copper–quinone complexes.[21] The cation shows a signal centered at $g = 2.003$ with no hyperfine in 1,2-dichloroethane solution at temperatures down to 77 K.[14] In the more polar solvents DMF or CH_3CN at low temperature, the signal can be resolved into $g_\parallel$ and $g_\perp$ components. Similar spectral results have been reported for Ru(II)–semiquinonate complexes containing phosphine and CO ligands.[22] The conclusion regarding charge distribution in the cationic complex from the combined information provided by the structural characterization and the EPR spectra is that it most closely resembles the Ru(II)–semiquinonate form. However, ambiquities in the results of both types of experiments make this assignment much less decisive than in the copper examples.

Options for charge distribution for a complex consisting of two quinone ligands chelated to ruthenium include $Ru^{IV}(Cat)_2$, $Ru^{III}(Cat)(SQ)$, and $Ru^{II}(SQ)_2$. The diamagnetism of $Ru(4\text{-}t\text{-}Bupy)_2(DBQ)_2$ and the sharp resolution of the ^1H NMR spectrum argue against a form with paramagnetic ligands.[15] $Cr(DBSQ)_3$,

(20) Bhattacharya, S.; Chakravorty, A.; Cotton, F. A.; Mukherjee, R.; Schwotzer, W. *Inorg. Chem.* **1984**, *23*, 1709.
(21) Buchanan, R. M.; Wilson-Blumenberg, C.; Trapp, C.; Larsen, S. K.; Greene, D. L.; Pierpont, C. G. *Inorg. Chem.* **1986**, *25*, 3070.
(22) Girgis, A. Y.; Sohn, Y. S.; Balch, A. L. *Inorg. Chem.* **1975**, *14*, 2327.

though diamagnetic due to coupling between paramagnetic ligands and the $S = {}^3/_2$ metal ion, shows only broad resonances for ligand *tert*-butyl groups, and $Pd(DBSQ)_2$ shows a similar NMR spectrum due to coupling between the paramagnetic ligands through the diamagnetic metal.[23] Further, the symmetrical equivalence of the quinone ligands in the structure of $Ru(t\text{-}Bupy)_2(DBQ)_2$ with the spherical shape of the thermal ellipsoids of ligand oxygens is inconsistent with a disordered mixed-charge ligand Ru(III) formulation. Cobalt and iron analogues, M(N–N)(DBSQ)(DBCat) (M = Co, Fe), have been reported with this charge distribution.[24,25] The $Ru^{IV}(Cat)_2$ option is consistent with the magnetic property of the complex and is in accord with the tendency for catecholate ligands to stabilize metals in high oxidation states, but the ligand C–O lengths are 0.02 Å shorter than the catecholate value. We conclude from this that there is no good localized charge formulation for the complex and that the electronic structure of the complex is best described in terms of a delocalized model similar to the 1,2-dithiolene complexes.[26] In other studies structural results usually coupled with spectral and magnetic properties have led to localized charge assignments for quinone and metal. This appears to represent the first situation where charge delocalization has been observed for quinone ligands.

Acknowledgment. This research was supported by the National Science Foundation under Grants CHE 85-03222 and CHE 84-12182 (X-ray instrumentation). We also thank Prof. A. B. P. Lever for samples of the compounds used in this study and for many stimulating discussions.

Supplementary Material Available: Tables containing anisotropic thermal parameters and bond distances and angles for $[Ru(bpy)_2(DBSQ)](ClO_4)$ and $Ru(t\text{-}Bupy)_2(DBQ)_2$ (6 pages); tables of structure factors for both compounds (28 pages). Ordering information is given on any current masthead page.

(23) Fox, G. A.; Pierpont, C. G., work in preparation.
(24) Buchanan, R. M.; Pierpont, C. G. *J. Am. Chem. Soc.* **1980**, *102*, 4951.
(25) Lynch, M. W.; Valentine, A.; Hendrickson, D. N. *J. Am. Chem. Soc.* **1982**, *104*, 6982.
(26) McCleverty, J. A. *Prog. Inorg. Chem.* **1968**, *10*, 49.

Contribution from the Department of Chemistry, University of California, Davis, California 95616

Synthesis and Spectroscopic and X-ray Structural Characterization and Dynamic Solution Behavior of the Neutral Cobalt(II) Alkoxides $[Co\{OC(C_6H_{11})_3\}_2]_2\cdot CH_3OH\cdot{}^1/_2C_6H_{12}\cdot THF$, $[Co(OCPh_3)_2]_2\cdot n\text{-}C_6H_{14}$, $[Co(OSiPh_3)_2(THF)]_2$, and $Co(OCPh_3)_2(THF)_2$

Gary A. Sigel, Ruth A. Bartlett, David Decker, Marilyn M. Olmstead, and Philip P. Power*

Received August 14, 1986

Reaction of the metal amide $[Co\{N(SiMe_3)_2\}_2]_2$ with the appropriate alcohol or silanol affords several examples of previously undescribed neutral cobalt alkoxides in moderate yields. These are the complexes $[Co\{OC(C_6H_{11})_3\}_2]_2\cdot CH_3OH\cdot{}^1/_2C_6H_{12}\cdot THF$ (**1**), $[Co(OCPh_3)_2]_2\cdot n\text{-}C_6H_{14}$ (**2**), $[Co(OSiPh_3)_2(THF)]_2$ (**3**), $Co(OCPh_3)_2(THF)_2$ (**4**), and $Co\{OC(4\text{-}MeC_6H_4)_3\}_2(THF)_2$ (**5**). Compounds **1**–**4**, which have been structurally characterized, are the first authenticated neutral cobalt(II) alkoxides. The structures of compounds **1** and **2** are dimeric with the cobalts bound to two bridging alkoxides and one terminal alkoxide ligand. Each cobalt has trigonal-planar geometry in addition to a central nonplanar Co_2O_4 core. The Co···Co distances (ca. 2.9 Å) are considerably longer than those found in similar amide complexes. In the binuclear complex **3** and the monomeric **4**, cobalt has a severely distorted tetrahedral geometry. Other interesting features include the formation of CH_3OH and C_6H_{12} in the preparation of **1** and the fluxional behavior of complexes **2**, **4**, and **5** in solution. A range of physical properties, including ^1H NMR, electronic, and IR spectra are also reported. A variable-temperature ^1H NMR study of **2** or its 4-methyl-substituted analogue $[Co\{OC(4\text{-}MeC_6H_4)_3\}_2]_2$ (**6**) (derived from **5**) showed that the signals due to the bridging and terminal ligands coalesced upon heating in C_7D_8 solution. Energy barriers of 57–58 kJ mol^{-1} were estimated on the basis of coalescence temperatures and spectral parameters. Crystallographic data with Mo Kα radiation (λ = 0.71069 Å) at 130 K: **1**, a = 13.359 (4) Å, b = 14.589 (5) Å, c = 23.054 (9) Å, α = 72.73 (3)°, β = 77.14 (3)°, γ = 64.86 (3)°, Z = 2, triclinic, space group $P\bar{1}$; **2**, a = 11.787 (4) Å, b = 13.336 (4) Å, c = 20.107 (5) Å, α = 81.50 (2)°, β = 80.07 (3)°, γ = 89.40 (3)°, Z = 2, triclinic, space group $P\bar{1}$; **3**, a = 14.203 (2) Å, b = 22.060 (5) Å, c = 22.269 (3) Å, β = 92.71 (1)°, Z = 4, monoclinic, space group $P2_1/n$; **4**, a = 18.994 (9) Å, b = 9.600 (9) Å, c = 23.421 (11) Å, β = 119.66 (3)°, Z = 4, monoclinic, space group $C2/c$. For **1**, R = 0.076, for **2**, R = 0.072, for **3**, R = 0.056, and for **4**, R = 0.054.

Introduction

As part of our continuing study of low-coordinate transition-metal complexes, we recently reported the synthesis and structural characterization of the lithium salts of monomeric three-coordinate ionic cobalt(II) alkoxide/amide complexes. These are the species $[Co(Cl)(OC\text{-}t\text{-}Bu_3)_2Li(THF)_3]$, $[Li(THF)_{4.5}][Co\{N(SiMe_3)_2\}(OC\text{-}t\text{-}Bu_3)_2]$, and $Li[Co\{N(SiMe_3)_2\}(OC\text{-}t\text{-}Bu_3)_2]$.[1] These compounds were the first structurally characterized cobalt alkoxides, and they all possess the rare trigonal-planar geometry at the cobalt center.[1,2] Other features include agostic interactions between ligand CH_3's and Co or Li, as well as the involvement of Cl^- as a bridging ligand between Li^+ and Co(II).[1] Since the use of lithium alkoxides as ligand-transfer agents invariably gave products that included either halide or lithium halide as part of the coordination sphere of an ionic complex, we decided to synthesize neutral cobalt alkoxides by the alcoholysis of a cobalt amide. With the very crowded alcohol $HOC\text{-}t\text{-}Bu_3$, although exchange occurred with $[Co\{N(SiMe_3)_2\}_2]_2$, we have not yet been able to isolate crystals of product suitable for X-ray study. However, with $HOC(C_6H_{11})_3$, $HOCPh_3$, $HOC(4\text{-}MeC_6H_4)_3$, and $HOSiPh_3$ the products illustrated in Scheme I can be readily isolated and crystallized.

Experimental Section

General Procedures. All reactions were performed by using modified Schlenk techniques under an inert atmosphere of N_2. Solvents were freshly distilled from drying agents and degassed twice before use. Solutions containing the $[Co\{OC(C_6H_{11})_3\}_2]_2$ complex were the most air-sensitive. The compounds $HOC(C_6H_{11})_3$, $HOCPh_3$, $HOC(4\text{-}MeC_6H_4)_3$, and $HOSiPh_3$ were purchased from Aldrich or Alfa and used as received; $[Co\{N(SiMe_3)_2\}_2]_2$ was synthesized by a literature procedure.[3] Products

(1) Olmstead, M. M.; Power, P. P.; Sigel, G. *Inorg. Chem.* **1986**, *25*, 1027.
(2) Bradley, D. C.; Hursthouse, M. B.; Newing, C. W.; Welch, A. J. *J. Chem. Soc., Chem. Commun.* **1972**, 872.

0020-1669/87/1326-1773$01.50/0